substitutional disorder are likely to be intimately coupled phenomena in the α' structure.

Crystals of the β form are polysynthetically twinned about (100) and the structure of each β twin orientation state is very similar to that of the corresponding orientation state of the disordered α' form, apart from the small monoclinic distortion of the β lattice; the α' modification can therefore be considered as a limiting case of the β form, when macroscopic twin domains decrease their size to dimensions of a few unit cells, and the monoclinic cell transforms to orthorhombic so that both orientation states can be fitted into a unique lattice (Catti & Gazzoni, 1983). Thus as the orientation difference between the two α' states increases as the Ca content grows (*cf. Positional disorder*), a critical composition close to pure Ca_2SiO_4 is reached when the two orientation states can no longer coexist on a microscopic scale and have to split into twin domains of the β phase. No simple structural explanation of this kind, however, can be devised for the α'/β phase boundary on the opposite (Sr-rich) side of the state diagram; in this case, only the above argument that positional disorder is stabilized somehow by substitutional disorder seems to be proposable.

This research was supported financially by the Consiglio Nazionale delle Richerche and by the Ministero Pubblica Istruzione, Roma.

References

AIZU, K. (1970). *Phys. Rev. B*, **2**, 754-772.
BRAGG, W. L. & WILLIAMS, E. J. (1934). *Proc. R. Soc. London Ser. A*, **151**, 540-566.
CATTI, M. & GAZZONI, G. (1983). *Acta Cryst.* B**39**, 679-684.
CATTI, M., GAZZONI, G. & IVALDI, G. (1983). *Acta Cryst.* C**39**, 29-34.
CATTI, M., GAZZONI, G., IVALDI, G. & ZANINI, G. (1983). *Acta Cryst.* B**39**, 674-679.
FINGER, L. W. & PRINCE, E. (1975). *Natl Bur. Stand. (US) Tech. Note* 854.
GROSSE, H. P. & TILLMANNS, E. (1974). *Cryst. Struct. Commun.* **3**, 599-602.
HUTTON, J. & NELMES, R. J. (1981). *J. Phys. C*, **14**, 1713-1736.
International Tables for X-ray Crystallography (1974). Vol. IV. Birmingham: Kynoch Press.
MCGINNETY, J. A. (1972). *Acta Cryst.* B**28**, 2845-2852.
MAIR, S. L. (1982). *J. Phys. C*, **15**, 25-36.
MUSTAFAEV, N. M., ILYUKHIN, V. V. & BELOV, N. V. (1965). *Kristallografiya*, **10**, 805-814.
NAVROTSKY, A. (1971). *Am. Mineral.* **56**, 201-211.
NAVROTSKY, A. & KLEPPA, O. J. (1967). *J. Inorg. Nucl. Chem.* **29**, 2701-2714.
NORTH, A. C. T., PHILLIPS, D. C. & MATHEWS, F. S. (1968). *Acta Cryst.* A**24**, 351-359.

Acta Cryst. (1984). B**40**, 544-549

Determination of the Structure Factors of Cu and Cu_3Au by the Intersecting Kikuchi-Line Method

BY H. MATSUHATA

Department of Materials Science and Technology, Graduate School of Engineering Sciences, Kyushu University, Kasuga-shi 816, *Japan*

Y. TOMOKIYO

HVEM LAB, Kyushu University, Fukuoka-shi 812, *Japan*

AND H. WATANABE AND T. EGUCHI

Department of Materials Science and Technology, Graduate School of Engineering Sciences, Kyushu University, Kasuga-shi 816, *Japan*

(*Received* 26 *September* 1983; *accepted* 27 *June* 1984)

Abstract

The intersecting Kikuchi-line method combined with the convergent-beam method was applied to Cu and Cu_3Au alloy in order to determine the structure factors of low-order reflections. Splittings of Kikuchi lines for higher-order reflections at intersections were observed so clearly using a high-voltage electron microscope that the separations could be measured. From the measured separations, the structure factors of low-order reflections were obtained by means of many-beam calculations based on the dynamical electron diffraction theory. The structure factors of Cu determined for reflections 111 and 200 are in good agreement with those determined by the critical-voltage method and X-ray diffraction. For Cu_3Au alloy, structure factors of both fundamental and superlattice reflections were determined. It is demonstrated that the intersecting Kikuchi-line method is useful for the estimation of the degree of order in a

0108-7681/84/060544-06$01.50

small and local region of the specimen. The effects of absorption of electrons on the separation of Kikuchi lines are also discussed in detail.

1. Introduction

Since the structure factors of an alloy depend on the composition, temperature factors and degree of order, we can obtain useful information from the structure factors. One of the important methods for determining structure factors in electron diffraction is to exploit the critical-voltage effect (Nagata & Fukuhara, 1967), by which the structure factors of low-order reflections can be obtained with an accuracy of 1%. However, the critical-voltage method has some disadvantages. For instance, the reflections to which the critical-voltage method is applicable are limited. Usually superlattice reflections of ordering alloys have no critical voltage and we cannot determine the long-range-order parameter by this method (see, for instance, Sinclair, Goringe & Thomas, 1975). On the other hand, the intersecting Kikuchi-line method (IKL method) proposed by Gjønnes & Høier (1971) has some advantages (Terasaki, Watanabe & Gjønnes, 1979) and is expected to be applicable to the determination of the order parameters. The IKL method has been applied to some oxides and semiconductors (Høier & Andersson, 1974; Watanabe, Andersson & Gjønnes, 1974; Terasaki, Watanabe & Gjønnes, 1977, 1979) in which clear Kikuchi lines can usually be observed. However, Kikuchi patterns from thin metal foils suffer from bending of the specimens and are not so clear, so that the method has not been applied to metals and alloys. In this paper we discuss the application of the IKL method to metals and alloys. In order to reduce the influence of bending in a thin metal specimen and to obtain clear Kikuchi patterns, the IKL method was combined with the convergent-beam electron diffraction technique. This improved method was applied to Cu. The scattering factors of low-order reflections were determined, and the values were compared with those obtained by the critical-voltage method in order to examine how accurate values can be obtained. Furthermore, this method was applied to Cu_3Au and the degree of long-range order of a local and small region, which cannot be estimated by the critical-voltage method or X-ray diffraction, was evaluated. The structure factor for fundamental reflection 200 was also evaluated by this method. Before the analysis one of the important factors for the reliability of this method, the influence of the absorption effect on Kikuchi patterns, is discussed in detail.

2. Kikuchi patterns of metals and alloys

High-order Kikuchi lines **g** and **g**+**h** split at the intersections with low-order Kikuchi lines −**h** and **h** when **g** and **g**+**h** satisfy the Bragg condition simultaneously. Fig. 1(*a*) shows a schematic drawing of the corresponding Kikuchi pattern. As the separation D depends strongly on the structure factor for the reflection **h**, we can determine this structure factor by an analysis of the separation. Fig. 1(*b*) shows the Kikuchi pattern of the $L1_2$-type structure schematically. Here **h** and −**h** are superlattice reflections and 2**h** and −2**h** are fundamental ones; the splits D_s and D'_s of Kikuchi lines **g** and **g**+**h** can be observed at the intersections with the Kikuchi lines −**h** and **h**. The separations D_s and D'_s depend on the structure factor of superlattice reflection **h**, so that we can determine the structure factor for reflection **h** by the measurement and analysis of these separations D_s or D'_s. The splits D_N and D'_N of Kikuchi lines **g** and **g**+2**h** can be seen at the intersections with Kikuchi line −2**h** or 2**h**. As it is deduced that D_N and D'_N similarly depend on the structure factor for fundamental reflection 2**h**, we can determine the structure factor for this fundamental reflection.

3. Experimental procedure

An alloy of composition Cu-24·2 at% Au, or nominally Cu_3Au, was made by melting together pure Cu and Au in vacuum. In order to obtain a disordered state the alloy was quenched from 873 K into iced brine, and an ordered state was obtained by annealing at 633 K for 21 d. Specimens of pure Cu and Cu_3Au were prepared by the usual electropolishing. Kikuchi patterns were obtained with the convergent-beam electron diffraction technique. Since the accuracy in the measurement of separation D is expected to be improved at a high accelerating voltage (Terasaki *et al.*, 1979), the IKL patterns were taken at 1017 kV for Cu, but those of Cu_3Au were taken at 761 kV to avoid the significant change of the degree of order due to the electron irradiation. The separations D of the Kikuchi lines were measured on enlarged prints. The

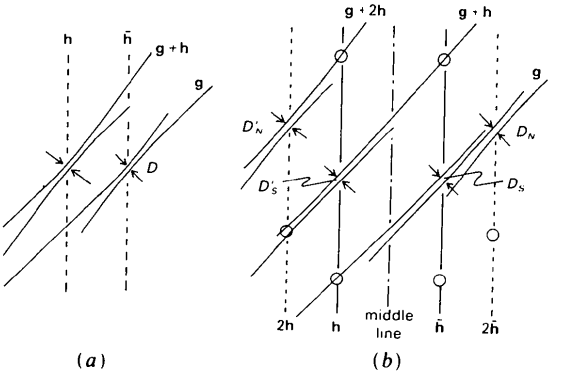

Fig. 1. Schematic drawing of intersecting Kikuchi lines (*a*) for pure f.c.c. crystals, (*b*) for $L1_2$-type ordering alloys. In fact, some other splits of Kikuchi lines can also be observed at the positions marked by circles.

analysis by the many-beam dynamical calculation was carried out with the eigenvalue method. In the calculation the atomic scattering factors given by Doyle & Turner (1968) for high-order reflections, the B factors of Cu_3Au given by Schwartz & Cohen (1965) and the ratios of the real and imaginary parts of the crystal potential V'_n/V_n given by Humphreys & Hirsch (1968) were used. The numbers of beams which were necessary for the calculation were examined similarly to Terasaki *et al.* (1979), and from 30 to 40 beams for Cu, and from 50 to 70 beams for Cu_3Au were considered for the analysis.

4. Results and discussion

(*a*) *Observation of Kikuchi patterns of* Cu

Fig. 2 shows an example of convergent-beam patterns taken from a relatively thin region (*a*) and a thick region (*b*) of a Cu crystal, where Kikuchi patterns and convergent-beam discs overlap each other. The Kikuchi lines can be seen outside and inside the discs. One can see in Fig. 2(*a*) that in the thick region segments 1 and 1′ of the split Kikuchi line are stronger in intensity than segments 2 and 2′. In the thin region, however, segments 1 and 1′ are weaker than 2 and 2′. In order to clarify the influence of the phenomenon on the splitting of the Kikuchi lines, intensity profiles of the Kikuchi lines along AB and $A'B'$ in Fig. 2 were calculated for the specimen with and without absorption. The calculated intensity profiles are shown in Fig. 3, where the attenuation of segments 1 and 1′, which is observed in Fig. 2, is well reproduced. The calculated results also indicate that the absorption has the effect of decreasing the separation D between the segments. But the decrease is found to be small compared with the actual experimental error for Cu; thus it can be ignored. As the Kikuchi pattern can be observed clearly in a properly thick crystal, such thickness is favorable for the observation of the separation of the Kikuchi lines of Cu. However, the effect of the thickness on D becomes significant for crystals with strong absorption such as the Cu_3Au alloy.

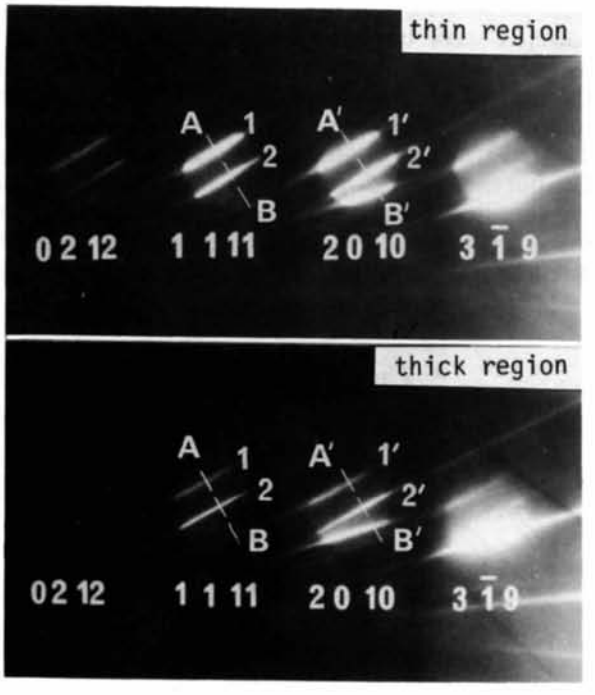

Fig. 2. Observed Kikuchi pattern of Cu taken from (*a*) thin, and (*b*) thick regions at 1017 kV, where $\mathbf{g}=2,0,10$ and $\mathbf{g}+\mathbf{h}=1,1,11$ satisfy the Bragg condition. The numbers are the notations of the split Kikuchi-line segments.

Table 1. *Separation of split Kikuchi lines and electron scattering factors of* Cu *for reflections* 111 *and* 200

h	$\bar{1}11$	020
g, **g**+**h**	2,0,10 1,1,11	179 199
D_g (10^{-2} nm^{-1})	1·016 ± 0·014	0·750 ± 0·011
f_h (10^{-1} nm)		
present	2·95 ± 0·06	2·69 ± 0·05
critical voltage	(*a*) 3·02 ± 0·05	2·68 ± 0·05
	(*b*) 3·01 ± 0·05	2·69 ± 0·05
X-ray	(*c*) 3·00 ± 0·03	2·72 ± 0·03

Notes: (*a*) Kuroda, Tomokiyo & Eguchi (1981). (*b*) Watanabe, Uyeda & Fukuhara (1969)(converted from X-ray scattering factors). (*c*) Takama & Sato (1982) (converted from X-ray scattering factors).

The measured separation D and the atomic scattering factors obtained are listed in Table 1, where the values obtained by the critical-voltage measurement are also shown for comparison. One can see that the accuracy of the present results is comparable with that obtained by the critical-voltage effect and X-ray diffraction. Goodman & Lehmpfuhl (1967) proposed

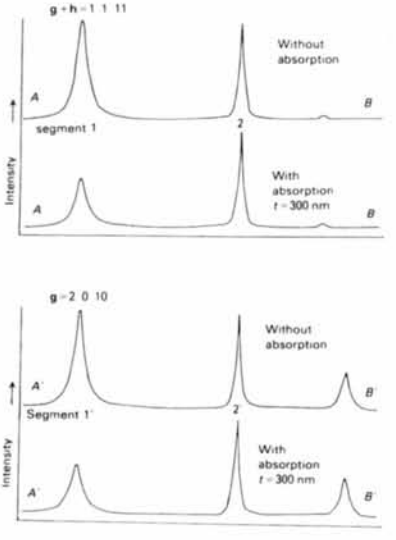

Fig. 3. Calculated profiles of split Kikuchi lines along AB and $A'B'$ in Fig. 2 with and without the absorption effect ($t = 300$ nm). Numbers correspond to the notations in Fig. 2.

a method for evaluating the structure factors by the convergent-beam technique. But their procedure is not easy to analyze compared with the present method. For the reasons mentioned above, we can conclude that the present method is satisfactorily applicable to metals and alloys for the estimation of structure factors.

(*b*) *Observation of the convergent-beam discs of* Cu_3Au

An example of the observed IKL patterns of an ordered Cu_3Au is shown in Fig. 4, where reflections $\bar{6}57$ and $\bar{7}57$ satisfy the Bragg condition simultaneously. The split Kikuchi lines and the fringe pattern due to elastic scattering overlap each other in the convergent-beam discs. Fig. 5 shows the calculated intensity profiles of Kikuchi lines $\bar{6}57$ and $\bar{7}57$ along AB and $A'B'$ in Fig. 4. The segments 1 and 1′ in Fig. 5 decay very rapidly with increase of thickness. In fact, in a thick crystal segments 1 and 1′ are broad and not clear. In a relatively thin crystal, as shown in Fig. 4, segments 1 and 1′ can be observed, but they are already broad. As the absorption effect is strong even in a thin crystal of Cu_3Au, the effect of absorption on the split Kikuchi line is discussed in detail.

(*c*) *Absorption effect*

As segments 1 and 1′ in Fig. 5 decay and have asymmetric profiles around the peaks in a thick crystal, the maximum position of the peak moves toward segment 2 or 2′. The absorption effect gives rise to a decrease in the separations D_s and D'_s. The effect of absorption on the split Kikuchi lines can be understood in terms of the behavior of Bloch waves. Figs. 6(*a*) and 6(*b*) illustrate the dispersion surfaces and intensity profiles of Bloch waves which contribute dominantly to the intensity of reflection $\bar{6}57$. Here, Bloch waves *A* and *B* attenuate very rapidly, so that the segments of Kikuchi lines 1 and 1′ become broad. Furthermore, as Bloch wave *A* decays more rapidly than Bloch wave *B*, segments 1 and 1′ become asymmetric in shape and the separation between segments 1 and 2, or 1′ and 2′ becomes narrow. When the imaginary part of the crystal potential is large, in

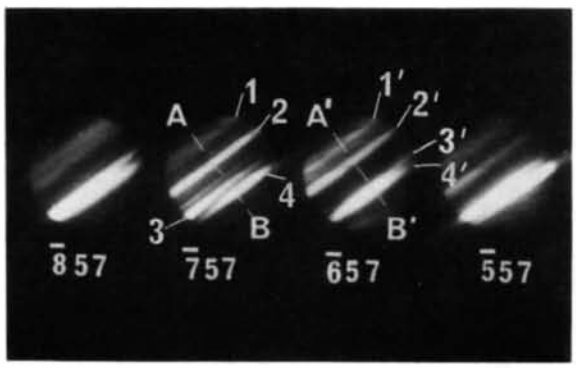

Fig. 4. Convergent-beam diffraction discs of an ordered Cu_3Au at 761 kV, where $\mathbf{g} = \bar{6}57$ and $\mathbf{g}+\mathbf{h} = \bar{7}57$ satisfy the Bragg condition. The Kikuchi pattern and the convergent-beam discs overlap each other. The splittings of Kikuchi lines D_s and D'_s due to superlattice reflection 100 can be observed. Numbers are the notations of the Kikuchi-line segments. In the convergent-beam discs not only Kikuchi lines but also some fringes due to the elastic scattering are observed.

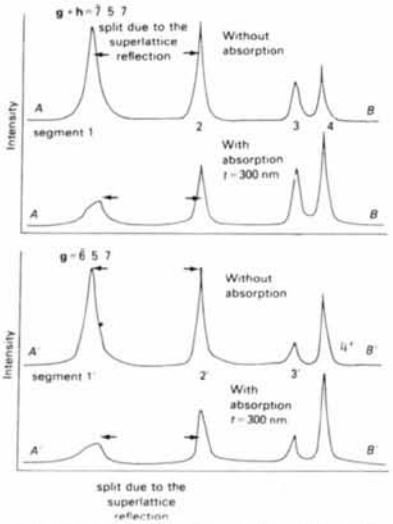

Fig. 5. Calculated intensity profiles of the Kikuchi pattern along AB and $A'B'$ in Fig. 4 with and without the absorption effect. The numbers are the notations of the Kikuchi-line segments, and correspond to those in Fig. 4.

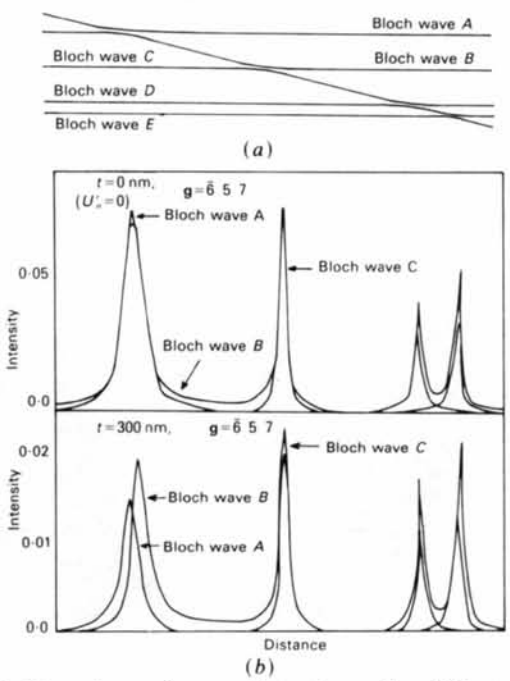

Fig. 6. Dispersion surfaces and intensity profiles of Bloch waves which dominantly contribute to reflection $\bar{6}57$ (*a*) without and (*b*) with the absorption effect at 300 nm thickness.

Table 2. *Separations of split Kikuchi lines for* Cu_3Au *and structure factors for reflections* 100 *and* 200

	Ordered Cu_3Au	Disordered Cu_3Au
$D_{\bar{6}57}$ (10^{-2} nm^{-1})	0·449 ± 0·031	
F^*_{100} (nm)	0·369 ± 0·024	
$D_{\bar{5}57}$ (10^{-2} nm^{-1})	0·549 ± 0·018	0·869 ± 0·036
F^*_{200} (nm)	1·28 ± 0·04	1·34 ± 0·07

* Includes temperature factors.

general the absorption coefficients of Bloch waves A and B also have correspondingly large values. The present calculation indicates that the amount of the decrease in the separation is 2% for the Cu_3Au crystal at thickness 300 nm, and 0·4% for Cu at thickness 300 nm. As the decrease in separation for the Cu_3Au alloy is comparable to the measurement error of the separation, the absorption effect cannot be ignored.

(*d*) *Structure factor for the superlattice reflection*

As the separations D_s and D'_s due to the superlattice reflection strongly depend on the structure factor for the superlattice reflection, we can estimate the degree of order S from the measurement of the separation. The absorption effect was considered and the thickness of the crystal was assumed to be 300 nm. This assumption of the thickness gives no serious error compared with the measurement error of D_s.

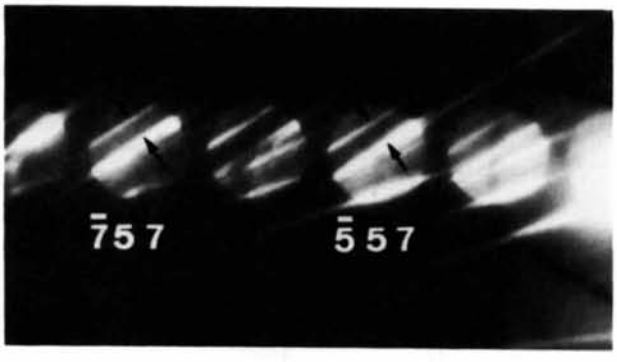

(*a*)

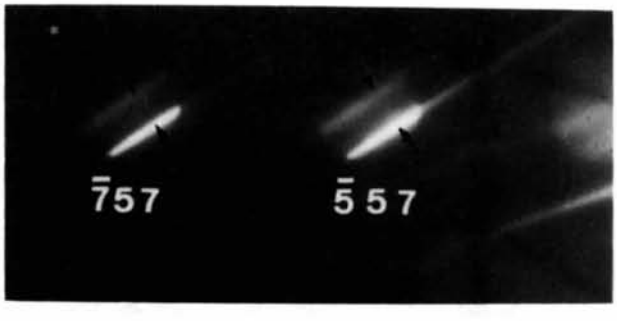

(*b*)

Fig. 7. Splitting of Kikuchi lines D_N and D'_N due to fundamental reflection 200, for (*a*) ordered and (*b*) disordered states of Cu_3Au at 761 kV. $\mathbf{g} = \bar{5}57$ and $\mathbf{g} + 2\mathbf{h} = \bar{7}57$ satisfy the Bragg condition.

The value of S obtained by the analysis of Fig. 4 is 0·84 ± 0·05, which is comparable with the value obtained with the similar heat treatment by Kinoshita, Mukai & Kitajima (1977) and that expected from Cowley's (1950) results. The structure factor for reflection 100 by the present analysis is shown in Table 2 together with the value of the measured D_s. In the case of Cu_3Au, segment 1 or 1′ is broad and not so clear due to the strong absorption effect. This gives a slightly large measurement error. However, by other diffraction methods, including the critical-voltage method and the X-ray diffraction, it is impossible to estimate the degree of order in a local and small region of a specimen.

(*e*) *Observation of the split Kikuchi lines due to the fundamental reflections*

The observed split Kikuchi lines due to the fundamental reflection 200 of the ordered and disordered states are shown in Figs. 7(*a*) and 7(*b*) respectively, where the separations D_N and D'_N become narrow on ordering. As the shape of the split Kikuchi pattern expresses a section of the dispersion surfaces, Fig. 7 shows how the shapes of the dispersion surfaces are changed by the appearance of superlattice reflections. Figs. 7(*a*) and 7(*b*) were analyzed to obtain the structure factor for 200, assuming that S is 0·84 for (*a*) and thickness t is 300 nm for (*a*) and (*b*). The results are summarized in Table 2. The structure factors for the reflection 200 obtained by the present study also have slightly large errors for the same reason as for reflection 100. Fig. 7 and Table 2 show that the separations D_N and D'_N also depend on the structure factor for reflection 100 as well as reflection 200 in an ordered state because of the many-beam effect. Therefore, we can obtain the degree of order from the separations D_N and D'_N, if the structure factor for the fundamental reflection is known beforehand.

This work was partly supported by a Grant in Aid for Scientific Research from the Ministry of Education.

References

COWLEY, J. M. (1950). *Phys. Rev.* **17**, 669–675.
DOYLE, P. A. & TURNER, P. S. (1968). *Acta Cryst.* A**24**, 390–397.
GJØNNES, J. & HØIER, R. (1971). *Acta Cryst.* A**27**, 313–316.
GOODMAN, P. & LEHMPFUHL, G. (1967). *Acta Cryst.* **22**, 14–24.
HØIER, R. & ANDERSSON, B. (1974). *Acta Cryst.* A**30**, 93–95.
HUMPHREYS, C. J. & HIRSCH, P. B. (1968). *Philos. Mag.* **18**, 115–122.
KINOSHITA, C., MUKAI, T. & KITAJIMA, S. (1977). *Acta Cryst.* A**33**, 605–609.
KURODA, K., TOMOKIYO, Y. & EGUCHI, T. (1981). *Trans. Jpn Inst. Met.* **22**, 535–542.
NAGATA, F. & FUKUHARA, A. (1967). *Jpn J. Appl. Phys.* **6**, 1233–1235
SCHWARTZ, L. H. & COHEN, J. B. (1965). *J. Appl. Phys.* **36**, 598–616.

SINCLAIR, R., GORINGE, M. J. & THOMAS, G. (1975). *Philos. Mag.* B32, 501-512.
TAKAMA, T. & SATO, S. (1982). *Philos. Mag.* B45, 615-625.
TERASAKI, O., WATANABE, D. & GJØNNES, J. (1977). *Proceedings of the Fifth International Conference on High-Voltage Electron Microscopy*, edited by T. IMURA & H. HASHIMOTO, pp. 263-266. Kyoto: Japanese Society of Electron Microscopy.
TERASAKI, O., WATANABE, D. & GJØNNES, J. (1979). *Acta Cryst.* A35, 895-900.
WATANABE, D., ANDERSSON, B. & GJØNNES, J. (1974). *Acta Cryst.* A30, 772-776.
WATANABE, D., UYEDA, R. & FUKUHARA, A. (1969). *Acta Cryst.* A25, 138-140.

Acta Cryst. (1984). B40, 549-554

High-Resolution Electron Microscopy Study of Polycrystalline Evaporated Titanium Monoxide Films

BY SHEN GUANG JUN AND L. A. BURSILL

School of Physics, University of Melbourne, Parkville, 3052 *Victoria, Australia*

K. YOSHIDA AND Y. YAMADA

College of General Education, Tohoku University, Kawauchi, Sendai 980, *Japan*

AND H. OTA

1*MV Electron Microscope Laboratory, Tohoku University, Katahira, Sendai* 980, *Japan*

(*Received* 6 *December* 1983; *accepted* 11 *June* 1984)

Abstract

High-resolution electron microscope (HREM) images of the δ phase of TiO_x ($0{\cdot}7 \le x \le 1{\cdot}0$) were analysed by comparison with computer-simulated images. This allowed a hexagonal structural model, proposed previously on the basis of powder X-ray data, to be confirmed using effectively single-crystal data for two projections of the structure. A study of the sensitivity of HREM images to crystal thickness and local variations in stoichiometry allowed (i) local variations in grain thickness to be assigned in the range 173 to 245 Å and (ii) the local stoichiometry to be assigned as $x = 0{\cdot}8$. The techniques developed should extend readily to studies of other polycrystalline thin films.

1. Introduction

The crystal structure of TiO_x ($0 \le x \le 1{\cdot}25$) varies with x, the Ti atom arrangement varying from essentially h.c.p. to essentially c.c.p. Thus the h.c.p. α phase occurs in the range $0 \le x \le 0{\cdot}5$, when oxygen atoms are included in tetrahedral interstices, and in the range $0{\cdot}5 \le x \le 0{\cdot}9$ a mixture of (α + TiO) phases may occur, depending upon thermal treatment (Roy & White, 1972). The Ti_2O phase represents one of the possible ordered arrangements of oxygen (Holmberg, 1962). The 'rock-salt' (c.c.p.) type TiO phase exists in the range $0{\cdot}7 \le x \le 1{\cdot}25$. This contains empty titanium and oxygen sites (Andersson, Collén, Kuglenstierna & Magnéli, 1957), which may become ordered following appropriate thermal treatments below 1260 K (Watanabe, Terasaki, Jostons & Castles, 1970). The so-called transition structure contains vacant sites of oxygen (Watanabe, Castles, Jostons & Malin, 1966) and titanium (Hilty, 1968) concentrated on every third (220) plane of the 'rock-salt' type structure. Such an ordering of space distorts the parent lattice (Hilty, 1968; Yamada 1983). The so-called δ phase may occur for $0{\cdot}53 \le x \le 0{\cdot}89$. Bumps, Kessler & Hansen (1953) reported its structure to be tetragonal, and this was apparently confirmed by Schofield & Bacon (1955-56). However, Andersson (1959) proposed a hexagonal structure for the δ phase. This was based upon an analysis of X-ray powder data. Since this phase apparently always coexists with α + TiO phases the structure analysis by single-crystal techniques was not possible. Yamada & Yoshida (1983) studied the phase transformation of evaporated films of $TiO_{0{\cdot}5}$ (α phase) into the TiO phase by *in situ* oxidation of evaporated thin films using an electron microscope, when a characteristic sequence of changes could be induced. Grains of the δ-phase precipitate during this transformation and Andersson's hexagonal unit-cell parameters for the δ phase were verified by analysing diffraction patterns taken from these single-crystal grains. The lattice parameters measured were nearly equal to those of Andersson, *i.e.* $A_\delta = 4{\cdot}99$ and $C_\delta = 2{\cdot}88$ Å.

In the present paper HREM images of the δ phase are presented for two projections of the structure.

0108-7681/84/060549-06$1.50